SELF-SUPERVISED LEARNING

Methods that make robots collect their own training data (with labels!) are called **self-supervised**. In this instance, the robot uses machine learning to leverage a short-range sensor that works well for terrain classification into a sensor that can see much farther. That allows the robot to drive faster, slowing down only when the sensor model says there is a change in the terrain that needs to be examined more carefully by the short-range sensors.

25.4 PLANNING TO MOVE

All of a robot's deliberations ultimately come down to deciding how to move effectors. The

POINT-TO-POINT MOTION

point-to-point motion problem is to deliver the robot or its end effector to a designated target

COMPLIANT MOTION

location. A greater challenge is the **compliant motion** problem, in which a robot moves while being in physical contact with an obstacle. An example of compliant motion is a robot manipulator that screws in a light bulb, or a robot that pushes a box across a table top.

We begin by finding a suitable representation in which motion-planning problems can be described and solved. It turns out that the **configuration space**—the space of robot states defined by location, orientation, and joint angles—is a better place to work than the original

PATH PLANNING

3D space. The **path planning** problem is to find a path from one configuration to another in configuration space. We have already encountered various versions of the path-planning problem throughout this book; the complication added by robotics is that path planning involves *continuous* spaces. There are two main approaches: **cell decomposition** and **skeletonization**. Each reduces the continuous path-planning problem to a discrete graph-search problem. In this section, we assume that motion is deterministic and that localization of the robot is exact. Subsequent sections will relax these assumptions.

25.4.1 Configuration space

We will start with a simple representation for a simple robot motion problem. Consider the robot arm shown in Figure 25.14(a). It has two joints that move independently. Moving the joints alters the (x, y) coordinates of the elbow and the gripper. (The arm cannot move in the z direction.) This suggests that the robot's configuration can be described by a four-dimensional coordinate: (x_e, y_e) for the location of the elbow relative to the environment and (x_g, y_g) for the location of the gripper. Clearly, these four coordinates characterize the full

WORKSPACE REPRESENTATION

state of the robot. They constitute what is known as **workspace representation**, since the coordinates of the robot are specified in the same coordinate system as the objects it seeks to manipulate (or to avoid). Workspace representations are well-suited for collision checking, especially if the robot and all objects are represented by simple polygonal models.

The problem with the workspace representation is that not all workspace coordinates are actually attainable, even in the absence of obstacles. This is because of the **linkage con-**

LINKAGE CONSTRAINTS

straints on the space of attainable workspace coordinates. For example, the elbow position (x_e, y_e) and the gripper position (x_g, y_g) are always a fixed distance apart, because they are joined by a rigid forearm. A robot motion planner defined over workspace coordinates faces the challenge of generating paths that adhere to these constraints. This is particularly tricky

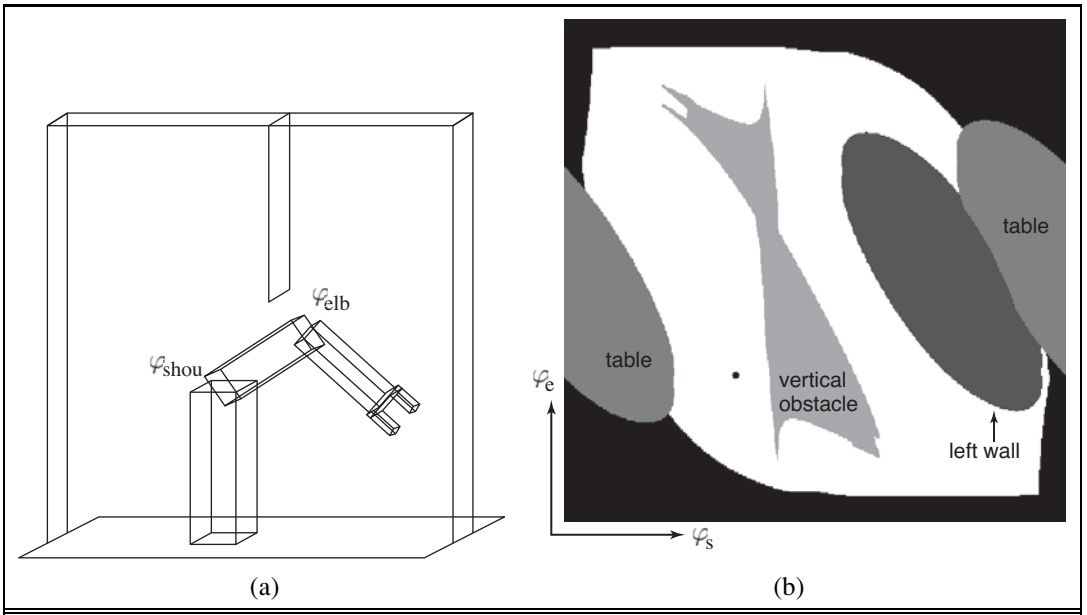

Figure 25.14 (a) Workspace representation of a robot arm with 2 DOFs. The workspace is a box with a flat obstacle hanging from the ceiling. (b) Configuration space of the same robot. Only white regions in the space are configurations that are free of collisions. The dot in this diagram corresponds to the configuration of the robot shown on the left.

CONFIGURATION SPACE

because the state space is continuous and the constraints are nonlinear. It turns out to be easier to plan with a **configuration space** representation. Instead of representing the state of the robot by the Cartesian coordinates of its elements, we represent the state by a configuration of the robot's joints. Our example robot possesses two joints. Hence, we can represent its state with the two angles φ_s and φ_e for the shoulder joint and elbow joint, respectively. In the absence of any obstacles, a robot could freely take on any value in configuration space. In particular, when planning a path one could simply connect the present configuration and the target configuration by a straight line. In following this path, the robot would then move its joints at a constant velocity, until a target location is reached.

Unfortunately, configuration spaces have their own problems. The task of a robot is usually expressed in workspace coordinates, not in configuration space coordinates. This raises the question of how to map between workspace coordinates and configuration space. Transforming configuration space coordinates into workspace coordinates is simple: it involves a series of straightforward coordinate transformations. These transformations are linear for prismatic joints and trigonometric for revolute joints. This chain of coordinate transformation is known as **kinematics**.

KINEMATICS

INVERSE KINEMATICS

The inverse problem of calculating the configuration of a robot whose effector location is specified in workspace coordinates is known as **inverse kinematics**. Calculating the inverse kinematics is hard, especially for robots with many DOFs. In particular, the solution is seldom unique. Figure 25.14(a) shows one of two possible configurations that put the gripper in the same location. (The other configuration would has the elbow below the shoulder.)

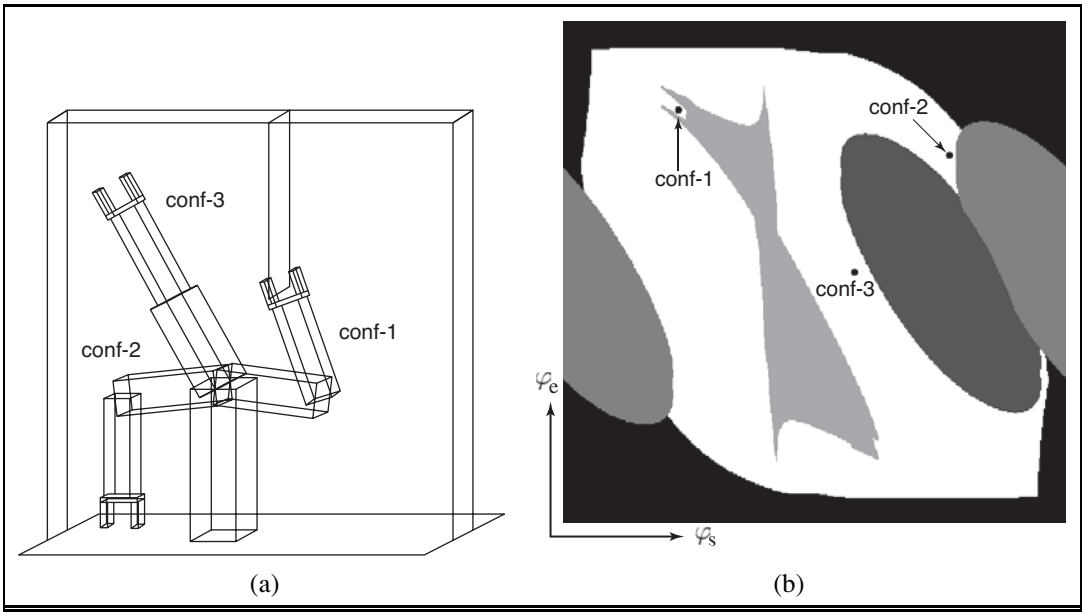

Figure 25.15 Three robot configurations, shown in workspace and configuration space.

In general, this two-link robot arm has between zero and two inverse kinematic solutions for any set of workspace coordinates. Most industrial robots have sufficient degrees of freedom to find infinitely many solutions to motion problems. To see how this is possible, simply imagine that we added a third revolute joint to our example robot, one whose rotational axis is parallel to the ones of the existing joints. In such a case, we can keep the location (but not the orientation!) of the gripper fixed and still freely rotate its internal joints, for most configurations of the robot. With a few more joints (how many?) we can achieve the same effect while keeping the orientation of the gripper constant as well. We have already seen an example of this in the "experiment" of placing your hand on the desk and moving your elbow. The kinematic constraint of your hand position is insufficient to determine the configuration of your elbow. In other words, the inverse kinematics of your shoulder–arm assembly possesses an infinite number of solutions.

The second problem with configuration space representations arises from the obstacles that may exist in the robot's workspace. Our example in Figure 25.14(a) shows several such obstacles, including a free-hanging obstacle that protrudes into the center of the robot's workspace. In workspace, such obstacles take on simple geometric forms—especially in most robotics textbooks, which tend to focus on polygonal obstacles. But how do they look in configuration space?

Figure 25.14(b) shows the configuration space for our example robot, under the specific obstacle configuration shown in Figure 25.14(a). The configuration space can be decomposed into two subspaces: the space of all configurations that a robot may attain, commonly called **free space**, and the space of unattainable configurations, called **occupied space**. The white area in Figure 25.14(b) corresponds to the free space. All other regions correspond to occu-

FREE SPACE

OCCUPIED SPACE

pied space. The different shadings of the occupied space corresponds to the different objects in the robot's workspace; the black region surrounding the entire free space corresponds to configurations in which the robot collides with itself. It is easy to see that extreme values of the shoulder or elbow angles cause such a violation. The two oval-shaped regions on both sides of the robot correspond to the table on which the robot is mounted. The third oval region corresponds to the left wall. Finally, the most interesting object in configuration space is the vertical obstacle that hangs from the ceiling and impedes the robot's motions. This object has a funny shape in configuration space: it is highly nonlinear and at places even concave. With a little bit of imagination the reader will recognize the shape of the gripper at the upper left end. We encourage the reader to pause for a moment and study this diagram. The shape of this obstacle is not at all obvious! The dot inside Figure 25.14(b) marks the configuration of the robot, as shown in Figure 25.14(a). Figure 25.15 depicts three additional configurations, both in workspace and in configuration space. In configuration conf-1, the gripper encloses the vertical obstacle.

Even if the robot's workspace is represented by flat polygons, the shape of the free space can be very complicated. In practice, therefore, one usually *probes* a configuration space instead of constructing it explicitly. A planner may generate a configuration and then test to see if it is in free space by applying the robot kinematics and then checking for collisions in workspace coordinates.

25.4.2 Cell decomposition methods

CELL DECOMPOSITION

The first approach to path planning uses **cell decomposition**—that is, it decomposes the free space into a finite number of contiguous regions, called cells. These regions have the important property that the path-planning problem within a single region can be solved by simple means (e.g., moving along a straight line). The path-planning problem then becomes a discrete graph-search problem, very much like the search problems introduced in Chapter 3.

The simplest cell decomposition consists of a regularly spaced grid. Figure 25.16(a) shows a square grid decomposition of the space and a solution path that is optimal for this grid size. Grayscale shading indicates the *value* of each free-space grid cell—i.e., the cost of the shortest path from that cell to the goal. (These values can be computed by a deterministic form of the VALUE-ITERATION algorithm given in Figure 17.4 on page 653.) Figure 25.16(b) shows the corresponding workspace trajectory for the arm. Of course, we can also use the A* algorithm to find a shortest path.

Such a decomposition has the advantage that it is extremely simple to implement, but it also suffers from three limitations. First, it is workable only for low-dimensional configuration spaces, because the number of grid cells increases exponentially with d, the number of dimensions. Sounds familiar? This is the curse!dimensionality@of dimensionality. Second, there is the problem of what to do with cells that are "mixed"—that is, neither entirely within free space nor entirely within occupied space. A solution path that includes such a cell may not be a real solution, because there may be no way to cross the cell in the desired direction in a straight line. This would make the path planner *unsound*. On the other hand, if we insist that only completely free cells may be used, the planner will be *incomplete*, because it might

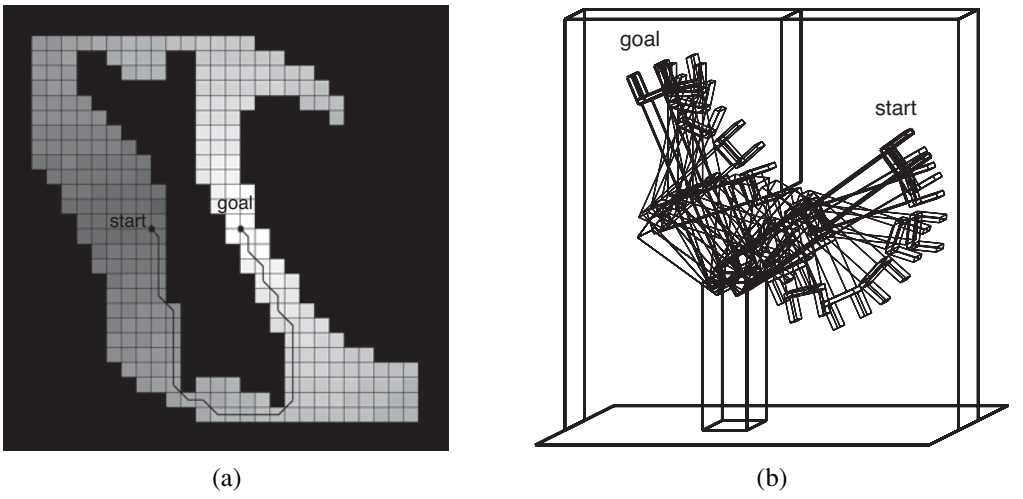

Figure 25.16 (a) Value function and path found for a discrete grid cell approximation of the configuration space. (b) The same path visualized in workspace coordinates. Notice how the robot bends its elbow to avoid a collision with the vertical obstacle.

be the case that the only paths to the goal go through mixed cells—especially if the cell size is comparable to that of the passageways and clearances in the space. And third, any path through a discretized state space will not be smooth. It is generally difficult to guarantee that a smooth solution exists near the discrete path. So a robot may not be able to execute the solution found through this decomposition.

Cell decomposition methods can be improved in a number of ways, to alleviate some of these problems. The first approach allows *further subdivision* of the mixed cells—perhaps using cells of half the original size. This can be continued recursively until a path is found that lies entirely within free cells. (Of course, the method only works if there is a way to decide if a given cell is a mixed cell, which is easy only if the configuration space boundaries have relatively simple mathematical descriptions.) This method is complete provided there is a bound on the smallest passageway through which a solution must pass. Although it focuses most of the computational effort on the tricky areas within the configuration space, it still fails to scale well to high-dimensional problems because each recursive splitting of a cell creates 2^d smaller cells. A second way to obtain a complete algorithm is to insist on an **exact cell decomposition** of the free space. This method must allow cells to be irregularly shaped where they meet the boundaries of free space, but the shapes must still be "simple" in the sense that it should be easy to compute a traversal of any free cell. This technique requires some quite advanced geometric ideas, so we shall not pursue it further here.

EXACT CELL DECOMPOSITION

Examining the solution path shown in Figure 25.16(a), we can see an additional difficulty that will have to be resolved. The path contains arbitrarily sharp corners; a robot moving at any finite speed could not execute such a path. This problem is solved by storing certain continuous values for each grid cell. Consider an algorithm which stores, for each grid cell,

the exact, continuous state that was attained with the cell was first expanded in the search. Assume further, that when propagating information to nearby grid cells, we use this continuous state as a basis, and apply the continuous robot motion model for jumping to nearby cells. In doing so, we can now guarantee that the resulting trajectory is smooth and can indeed be executed by the robot. One algorithm that implements this is **hybrid A***.

HYBRID A*

25.4.3 Modified cost functions

Notice that in Figure 25.16, the path goes very close to the obstacle. Anyone who has driven a car knows that a parking space with one millimeter of clearance on either side is not really a parking space at all; for the same reason, we would prefer solution paths that are robust with respect to small motion errors.

POTENTIAL FIELD

This problem can be solved by introducing a **potential field**. A potential field is a function defined over state space, whose value grows with the distance to the closest obstacle. Figure 25.17(a) shows such a potential field—the darker a configuration state, the closer it is to an obstacle.

The potential field can be used as an additional cost term in the shortest-path calculation. This induces an interesting tradeoff. On the one hand, the robot seeks to minimize path length to the goal. On the other hand, it tries to stay away from obstacles by virtue of minimizing the potential function. With the appropriate weight balancing the two objectives, a resulting path may look like the one shown in Figure 25.17(b). This figure also displays the value function derived from the combined cost function, again calculated by value iteration. Clearly, the resulting path is longer, but it is also safer.

There exist many other ways to modify the cost function. For example, it may be desirable to *smooth* the control parameters over time. For example, when driving a car, a smooth path is better than a jerky one. In general, such higher-order constraints are not easy to accommodate in the planning process, unless we make the most recent steering command a part of the state. However, it is often easy to smooth the resulting trajectory after planning, using conjugate gradient methods. Such post-planning smoothing is essential in many real-world applications.

25.4.4 Skeletonization methods

SKELETONIZATION

The second major family of path-planning algorithms is based on the idea of **skeletonization**. These algorithms reduce the robot's free space to a one-dimensional representation, for which the planning problem is easier. This lower-dimensional representation is called a **skeleton** of the configuration space.

VORONOI GRAPH

Figure 25.18 shows an example skeletonization: it is a **Voronoi graph** of the free space—the set of all points that are equidistant to two or more obstacles. To do path planning with a Voronoi graph, the robot first changes its present configuration to a point on the Voronoi graph. It is easy to show that this can always be achieved by a straight-line motion in configuration space. Second, the robot follows the Voronoi graph until it reaches the point nearest to the target configuration. Finally, the robot leaves the Voronoi graph and moves to the target. Again, this final step involves straight-line motion in configuration space.

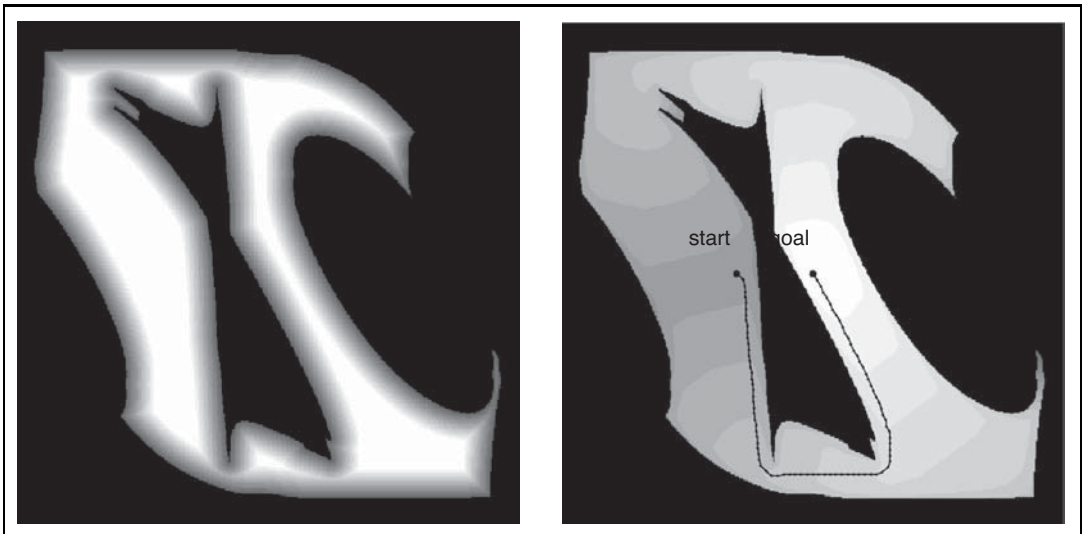

(a) (b)

Figure 25.17 (a) A repelling potential field pushes the robot away from obstacles. (b) Path found by simultaneously minimizing path length and the potential.

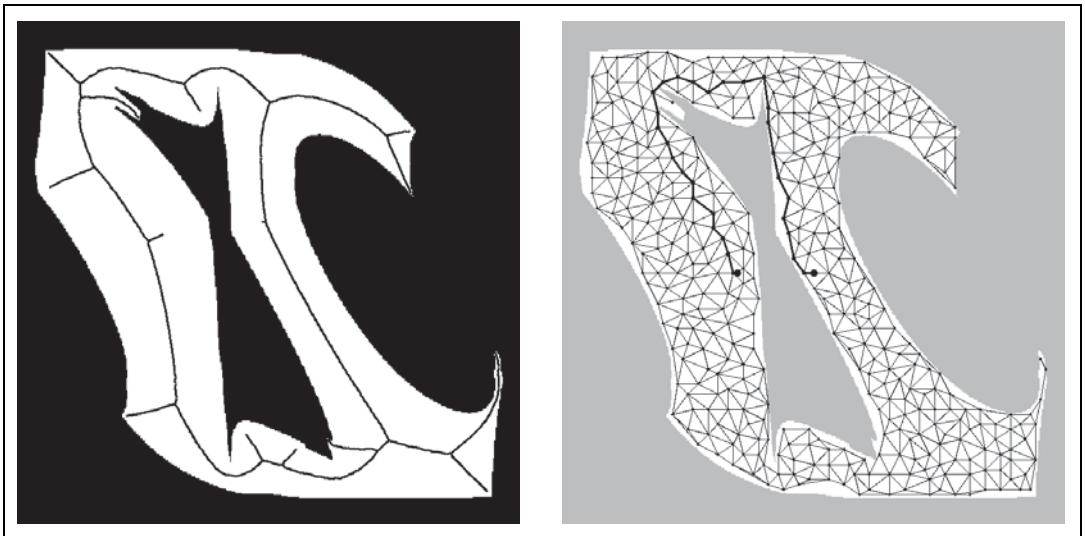

(a) (b)

Figure 25.18 (a) The Voronoi graph is the set of points equidistant to two or more obstacles in configuration space. (b) A probabilistic roadmap, composed of 400 randomly chosen points in free space.

In this way, the original path-planning problem is reduced to finding a path on the Voronoi graph, which is generally one-dimensional (except in certain nongeneric cases) and has finitely many points where three or more one-dimensional curves intersect. Thus, finding

the shortest path along the Voronoi graph is a discrete graph-search problem of the kind discussed in Chapters 3 and 4. Following the Voronoi graph may not give us the shortest path, but the resulting paths tend to maximize clearance. Disadvantages of Voronoi graph techniques are that they are difficult to apply to higher-dimensional configuration spaces, and that they tend to induce unnecessarily large detours when the configuration space is wide open. Furthermore, computing the Voronoi graph can be difficult, especially in configuration space, where the shapes of obstacles can be complex.

PROBABILISTIC ROADMAP

An alternative to the Voronoi graphs is the **probabilistic roadmap**, a skeletonization approach that offers more possible routes, and thus deals better with wide-open spaces. Figure 25.18(b) shows an example of a probabilistic roadmap. The graph is created by randomly generating a large number of configurations, and discarding those that do not fall into free space. Two nodes are joined by an arc if it is "easy" to reach one node from the other–for example, by a straight line in free space. The result of all this is a randomized graph in the robot's free space. If we add the robot's start and goal configurations to this graph, path planning amounts to a discrete graph search. Theoretically, this approach is incomplete, because a bad choice of random points may leave us without any paths from start to goal. It is possible to bound the probability of failure in terms of the number of points generated and certain geometric properties of the configuration space. It is also possible to direct the generation of sample points towards the areas where a partial search suggests that a good path may be found, working bidirectionally from both the start and the goal positions. With these improvements, probabilistic roadmap planning tends to scale better to high-dimensional configuration spaces than most alternative path-planning techniques.

25.5 Planning Uncertain Movements

None of the robot motion-planning algorithms discussed thus far addresses a key characteristic of robotics problems: *uncertainty*. In robotics, uncertainty arises from partial observability of the environment and from the stochastic (or unmodeled) effects of the robot's actions. Errors can also arise from the use of approximation algorithms such as particle filtering, which does not provide the robot with an exact belief state even if the stochastic nature of the environment is modeled perfectly.

Most of today's robots use deterministic algorithms for decision making, such as the path-planning algorithms of the previous section. To do so, it is common practice to extract the **most likely state** from the probability distribution produced by the state estimation algorithm. The advantage of this approach is purely computational. Planning paths through configuration space is already a challenging problem; it would be worse if we had to work with a full probability distribution over states. Ignoring uncertainty in this way works when the uncertainty is small. In fact, when the environment model changes over time as the result of incorporating sensor measurements, many robots plan paths online during plan execution. This is the **online replanning** technique of Section 11.3.3.

MOST LIKELY STATE

ONLINE REPLANNING